PAPER • OPEN ACCESS

Deconvolution-based methods to extract uncertainty components

OPEN ACCESS
IOP Publishing
Measurement Science and Technology
Meas. Sci. Technol. **35** (2024) 015036 (13pp)
https://doi.org/10.1088/1361-6501/ad0519

Deconvolution-based methods to extract uncertainty components

Alessandro Ferrero*, Simona Salicone, Harsha Vardhana Jetti and Sina Ronaghi

Politecnico di Milano, DEIB—Dipartimento di Elettronica, Informazione e Bioingegneria, P.za Leonardo da Vinci 32, 20133 Milano, Italy

E-mail: alessandro.ferrero@polimi.it

Received 13 January 2023, revised 6 August 2023
Accepted for publication 19 October 2023
Published 26 October 2023

Abstract

A measurement result is supposed to provide information about the distribution of values that could reasonably be attributed to the measurand. However, in general, it provides the distribution of values returned by the employed measuring system, when the measurand is given as the input quantity to this system. This distribution of values is mathematically given by the convolution of two probability density functions (PDFs): the one representing the actual distribution of values of the measurand and the one representing the uncertainty contribution of the employed measuring system. In principle, if the uncertainty contribution of the measuring system is known, the distribution of values that could reasonably be attributed to the measurand can be obtained by applying a proper deconvolution algorithm: this distribution is, indeed, the one of interest in any industrial measurement process. Similarly, if the PDF representing the distribution of values of the measurand is known, the PDF representing the uncertainty contribution of the measuring system to the resulting distribution of values returned by the instrument can be obtained by applying a proper deconvolution algorithm: this distribution is, indeed, the one of interest when a calibration is performed. In practical situations, deconvolution algorithms provide rather inaccurate results when applied to PDFs, especially when they are experimentally obtained from histograms of collected data. This paper proposes a deconvolution method, based on the use of Fuzzy variables (or Possibility Distributions) to represent distribution of values, which proves to provide much more accurate results. Simulation results, as well as experimental results are discussed to validate the proposed method.

Keywords: uncertainty, deconvolution, random-fuzzy variables, *a priori* distribution, probability distributions, possibility distributions

1. Introduction

It is well-known, in metrology, that a measurement result is a *set of quantity values being attributed to a measurand together with any other available relevant information*, so that it may convey '*relevant information' about the set of quantity values, such that some may be more representative of the measurand than others and this may be expressed in the form of a probability density function (PDF)* [1]. Such relevant information is generally expressed in terms of measurement uncertainty that, according to the GUM [2], *should provide an interval about the measurement result that may be expected to encompass a large fraction of the distribution of values that could reasonably be attributed to the quantity subject to measurement* and such an interval can be readily provided if the PDF representing such distribution of values is known or assumed.

* Author to whom any correspondence should be addressed.

However, it is also known that a measurement procedure of a generic measurand X cannot provide the distribution of values that can reasonably be attributed to random variable X, but, because of the uncertainty contribution introduced by the measuring system, it estimates the distribution of values Y that can be assigned to the values returned by the measuring system itself. Therefore, if S represents the intrinsic variability of the employed measuring system, the output of the measurement procedure is represented, mathematically, by random variable [3]:

$$Y = X * S \tag{1}$$

where symbol $*$ represents the mathematical convolution between two random variables.

It can be readily checked that, unless the measuring system's variability is negligible with respect to the measurand's variability, measurement result Y does not actually represent measurand X and this difference may make the measurement result useless. This is the case when the variability of a product of an industrial production must be evaluated or when the measurement result must be used to assess conformity of a product [4]. In such a situation, if S is known, it is possible, in principle, to obtain X by means of a deconvolution operation, as:

$$X = \frac{Y}{S}. \tag{2}$$

A similar situation occurs during calibration operations, when a reference X with known variability is employed to evaluate the variability S of the measuring system under calibration. In this case, the measurement result Y would not correctly represent S, unless the variability of X be negligible with respect to S. Since this is not always the case, S can be obtained, similarly to the previous case, by means of a deconvolution operation, as:

$$S = \frac{Y}{X}. \tag{3}$$

While deconvolution appears to be a powerful theoretical tool to extract the information of interest (X with (2), or S with (3)) from the measurement result Y, its practical utility is limited to the case when Y, X and S can be represented by normal PDFs, and the mean value and variance of the deconvolved PDF can be obtained in closed form. In all other cases, and in particular when the PDFs are obtained from a series of experimental data or estimated by means of a Monte Carlo simulation [5], a deconvolution algorithm must be used and the result is, generally, a poor approximation of the desired PDF.

Recently, the use of possibility distributions (PDs) has been proposed to represent variability and, specifically, measurement results, as an alternative way, compliant with the GUM principles [6–10], to the representation of measurement results in term of PDFs. An interesting outcome of such a representation is that operations among PDs, including convolution and deconvolution, require only algebraic computations, thus providing, in general, much better results than the same operations performed on PDFs.

This paper, after having briefly recalled some of the most used available methods to perform a deconvolution of two PDFs, will briefly recall the definition of PDs and how and under which conditions a PDF can be transformed into a corresponding PD, and will then show how convolution and deconvolution of PDs can be performed. The capability of PDs to provide accurate deconvolution results will be proved by means of simulations and the proposed method is then validated experimentally, by retrieving the PD representing the measurand's variability from the measurement result, given that the contribution of the employed measuring system known.

2. Deconvolution of probability distributions

Let X and Y be two generic vectors of size N. The convolution[2] between them is given by:

$$Z(i) = X(i) * Y(i) = \sum_{k=0}^{N} X(i)\, Y(i-k)\,. \tag{4}$$

When vectors X and Y are obtained from normal PDFs, their convolution is obtained in a fairly simple way as a normal PDF whose mean value and variance are computed by adding the mean values and variances of the two initial PDFs.

The inverse operation of convolution (4) is called a deconvolution and returns either X, given Z and Y, or Y, given Z and X. The adopted notation is, respectively:

$$X = \frac{Z}{Y}. \tag{5}$$

$$Y = \frac{Z}{X}. \tag{6}$$

Once again, when all vectors are obtained from normal PDFs, the deconvolution result is a normal PDF, whose mean value and variance are simply obtained by calculating the difference between the mean values and variances of the initial PDFs.

When different PDFs from the normal ones are considered, there is no mathematical closed form solution to the deconvolution operation. Hence, specific algorithms must be used, that mostly work in an iterative way, as the ones proposed in [11–17]. In particular, the blind deconvolution algorithm proposed in [11–13] appears to be quite interesting, since no assumption is needed on X and Y. This is the case when X and Y are obtained either from a series of experimental data or a Monte Carlo simulation and cannot be represented by a known equation. With a blind deconvolution algorithm both the original vectors (X and Y) are estimated by maximizing the likelihood that the two estimated vectors when convolved provide the initial vector (Z).

[2] In this paper only the discrete convolution is considered, since it is assumed that, in practice, only a discrete number of calibrations is available.

A non-blind deconvolution algorithm, the Lucy–Richardson algorithm, was proposed in [14, 15]. This algorithm assumes that the convolved vector (Z) and one of the two original vectors (either X or Y) are known and the deconvolution is again based on maximizing the likelihood that the estimated vector when convolved with the known original vector, provides the convolved vector (Z).

Another non-blind algorithm, based on the Wiener filter, was proposed in [16, 17]. Also this algorithm assumes some prior knowledge of one of the two original vectors (X or Y) is known.

All deconvolution algorithms are directly applied on the vectors. Since they are iterative in nature, aimed at minimizing an objective function, they provide an approximate solution to the deconvolution, and the approximation can be rather poor: this is probably the main drawback in deconvolving PDFs directly using the deconvolution algorithms.

3. The PDs

3.1. Definition

As already mentioned in section 1, a rather recent mathematical theory, the theory of possibility, has been proposed in the literature [6–10] as an alternative method to the theory of probability, to represent incomplete knowledge. This theory is based on the more general mathematical theory of evidence [18], that encompasses, as particular cases, both possibility and probability.

Without entering into too many mathematical details, let us very briefly recall the definition of a PD. A PD is a convex function $r_X(x)$, such that $r : X \to [0,1]$ and $sup_{x\in X} r_X(x) = 1$ [18]. The cuts I_α of a PD are called α-cuts and are defined as:

$$I_\alpha = \{x | r(x) \geqslant \alpha\}. \tag{7}$$

They can be considered as a generalization of the probabilistic concept of confidence intervals and a credibility can be associated to each of them, in the range $[0,1]$, that an element x belongs to them. In particular, the credibility value is given, for each α-cut at level α, by $1-\alpha$ [6].

Therefore, a PD can be represented by a set of α-cuts at the different possible levels α as shown in figure 1. An interesting property of the PDs is that their combination by means of mathematical operations like sum, difference, product, can be performed on their α-cuts by applying suitable triangular norms (t-norms) [6, 19–24].

3.2. PDF transformation into corresponding PDs

Unimodal probability distributions can be transformed into a corresponding PD distribution by applying suitable probability–possibility (p–p) transformations [6, 25–28]. The principle underlying these transformations is that the coverage probability p assigned to a given interval in the probability domain shall become the credibility assigned to the α-cut with the same width as the considered interval in probability. Therefore, such an α-cut is located, in the PD, at level $\alpha = 1-p$ [6, 27].

Examples of different PDs and the corresponding probability distributions obtained from the p–p transformation proposed in [6, 27] are shown in figures 2 and 3.

The advantage of the employed p-p transformation is that, since it operates on intervals of confidence with known levels of confidence, it can be applied also when the initial PDF is represented by an histogram of the distribution of experimental data or data obtained by means of a Monte Carlo simulation.

3.3. Convolution and deconvolution in the possibility domain

The most relevant advantage of representing a random variable with a corresponding PD, instead of a PDF, is that the convolution of two random variables is obtained by summing the PDs associated with the random variables [19, 20]. This means that, if X_{PD} and Y_{PD} are the PDs corresponding to random variable X and Y respectively, the PD representing their convolutions (Z_{PD}) is given by:

$$Z_{\{\mathrm{PD}\}} = X_{\mathrm{PD}} + Y_{\mathrm{PD}}. \tag{8}$$

Consequently, the deconvolution operation can be immediately performed as a difference of two PDs, the one representing the convolved distribution and the one representing one of the distributions that contributed to the convolution. This means that the PD X_{PD} can be obtained from the PDs, Z_{PD} and Y_{PD} as:

$$X_{\mathrm{PD}} = Z_{\mathrm{PD}} - Y_{\mathrm{PD}}. \tag{9}$$

A similar equation can be written for Y_{PD}.

4. The proposed method

The proposed method considers using PDs to represent the distributions of values X and S considered in section 1.

Considering the same meaning as those assigned to the symbols in section 1, let X represent the variability of the measurand, and let S represent the variability introduced by the measuring system's uncertainty. The distribution of values returned by the instrument systems' output is therefore represented, in the probability domain, by the following PDF:

$$Y(x) = \int_{-\infty}^{+\infty} X(x) \cdot S(t-x)\,\mathrm{d}t \tag{10}$$

or, if the PDFs are represented in the discrete domain with vectors of N elements, by:

$$Y(i) = X(i) * S(i) = \sum_{k=0}^{N} X(i) \cdot S(i-k). \tag{11}$$

Let us now suppose that, given Y and knowing S, X is desired: it can be obtained by performing the deconvolution

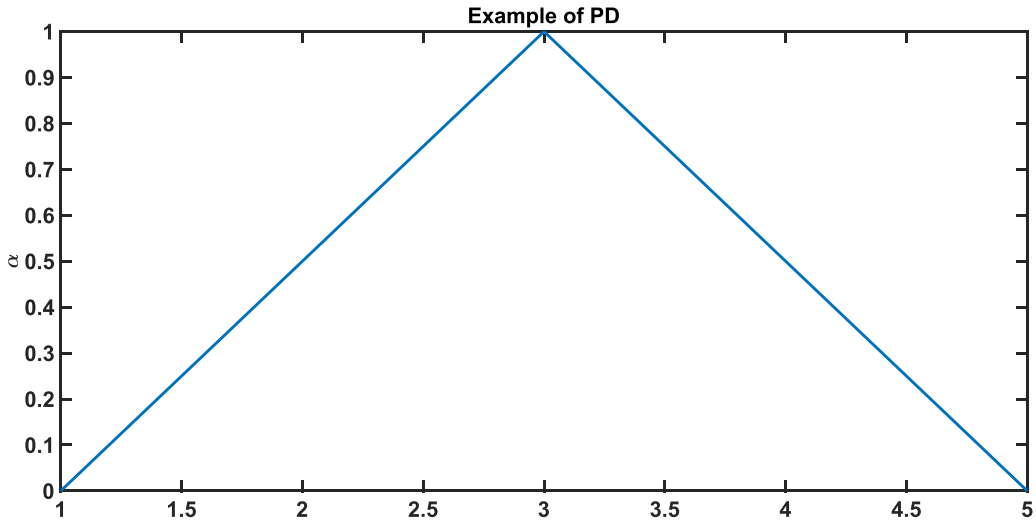

Figure 1. Example of possibility distribution centered on 3, whose α-cut in $\alpha = 0$ has width equal to 4.

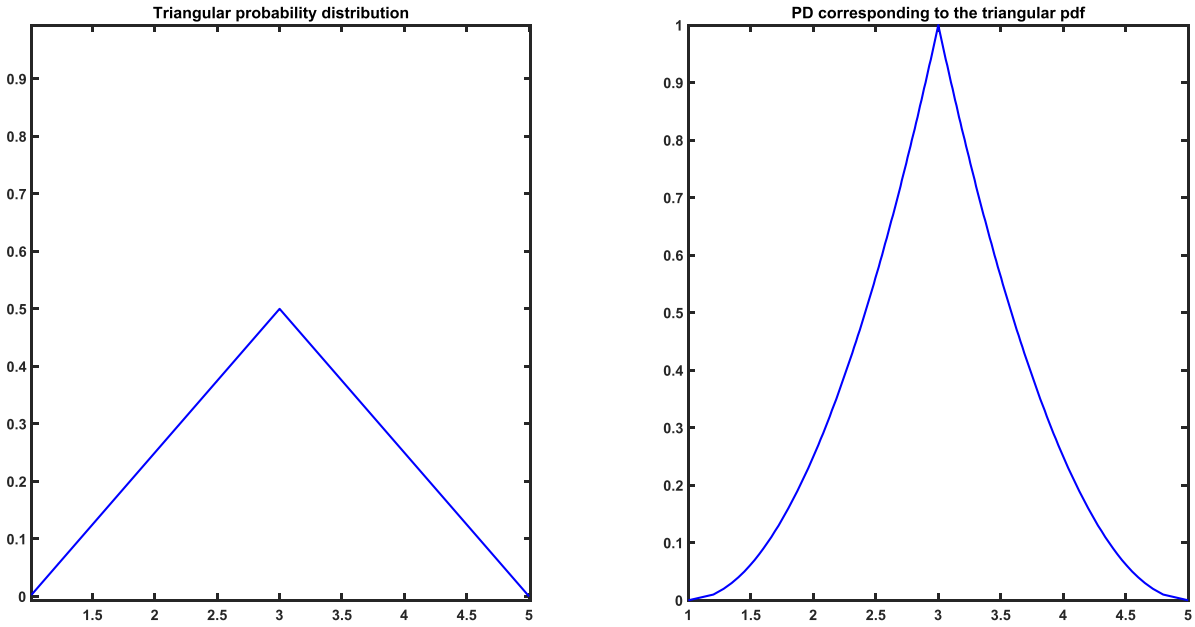

Figure 2. Triangular probability distribution and the corresponding possibility distribution.

of Y and S. This operation can be performed on the assumed probability distributions by applying the blind deconvolution algorithm [11–13], the Lucy–Richardson algorithm [14, 15] and the Wiener-filter algorithm [16, 17].

The same probability distributions assumed by these algorithm have been transformed into the corresponding Y_{PD}, X_{PD}, and S_{PD} PDs. The deconvolution algorithm is then performed in the possibility domain, where $X_{\mathrm{PD}} = Y_{\mathrm{PD}} - S_{\mathrm{PD}}$, and this difference is performed by applying the generalized Dombi t-norm that combines N generic r_i PDs according to the following equation [6, 29]:

$$T^{GDO}_{\gamma_1,\gamma_2}(r) = \frac{1}{1+\left(\frac{1}{\gamma_1}\left(\prod_{i=1}^{N}\left(1+\gamma_1\left(\frac{1-r_i}{r_i}\right)^{\gamma_2}\right)-1\right)\right)^{\frac{1}{\gamma_2}}} \tag{12}$$

where $\gamma_1 = 1.1$ and $\gamma_2 = 1.7$ [6].

In order to compare the results provided by the deconvolution algorithms working in the probability domain with the result provided by the deconvolution in the possibility domain in a homogenous way, the deconvolved PDFs obtained in the probability domain have been also transformed into a PD, so that the comparison can be performed in the possibility domain.

5. Simulation and simulation results

As a case study, a typical scenario is considered where a manufacturing process is being evaluated in an industry that produces resistors. In this scenario, the variability of the measuring instrument and the variability of the manufacturing process are assumed to be comparable, since, as shown in section 1,

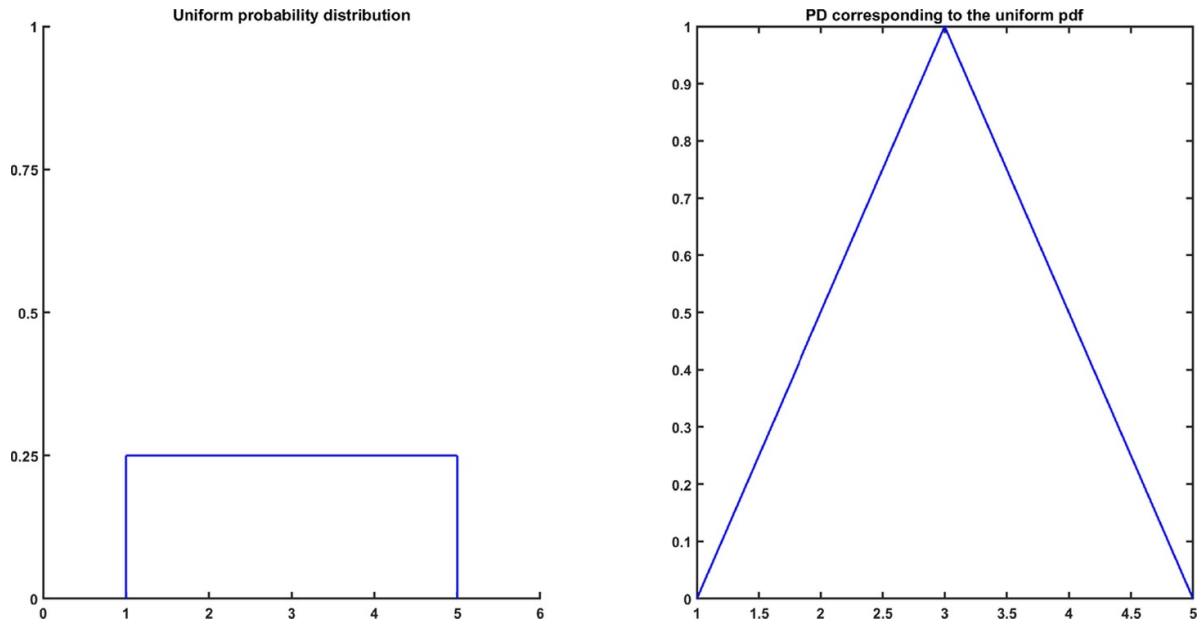

Figure 3. Uniform probability distribution and the corresponding possibility distribution.

this is the one that would provide the greatest difference between the actual process variability and the measured one.

Two cases have been considered with different types of probability distributions for the instrument and the manufacturing process. For each case, the proposed method of converting the probability distributions to PDs and then performing the difference of the PDs has been used and the comparison of the obtained results have been performed with the existing deconvolution methods by converting the obtained PDF after deconvolution into a PD.

5.1. Case 1

In case 1, it has been assumed that the industry is a resistor manufacturer and 15Ω resistors are being manufactured. It is assumed that the manufactured resistors distribute according to a uniform probability distribution X centered on 15Ω and with a half-width of 0.025Ω. Hence, X is given by,

$$X = U[14.975; 15.025)]\,. \tag{13}$$

It has been assumed that the variability S of the measuring instrument shows a uniform probability distribution as well, with a half-width of 0.0125Ω.

It has been assumed that 200 000 resistors have been measured using this instrument. So, to simulate the measuring process, the true value of the resistors (R_{true}) was obtained by drawing a random value from distribution X and then the measured value of the resistor is obtained by drawing a random value from the uniform distribution centered at each generated true value of the resistor and with a half-width of 0.0125Ω which is the probability distribution represented by $[R_{\text{true}} - 0.0125; R_{\text{true}} + 0.0125]$.

Therefore, 200 000 measured values have been obtained and their histogram has been generated to represent the distribution Y of the measurement results. Since the deconvolution algorithms require the PDFs expressed as functions, the histogram has been interpolated with a suitable fitting function to obtain the required functions. It was then possible to obtain distribution X_d from Y and S by applying one of the deconvolution algorithms seen in section 2. All considered PDFs have also been transformed into the corresponding PDs, and the proposed deconvolution algorithm applied.

Figure 4 shows the result of the comparison of the proposed method with that obtained from the blind deconvolution algorithm [11–13].

The red line represents the PD corresponding to the assumed X distribution, the blue line corresponds to the PD obtained from the X_d probability distribution after deconvolution using the blind deconvolution algorithm, and the green line represents the PD obtained using the proposed algorithm.

It can be clearly seen that the PD obtained using the proposed method is much closer to the actual X distribution than that obtained using the blind convolution algorithm.

Figure 5 shows the result of the comparison of the proposed method with that obtained from the Lucy–Richardson deconvolution algorithm [14, 15].

The red line represents the PD corresponding to the assumed X distribution, the blue line corresponds to the PD obtained from the X_d probability distribution after deconvolution using the Lucy–Richardson deconvolution algorithm, and the green line represents the PD obtained using the proposed algorithm.

It can be clearly seen that the PD obtained using the proposed method is much closer to the actual X distribution than that obtained using the Lucy–Richardson deconvolution.

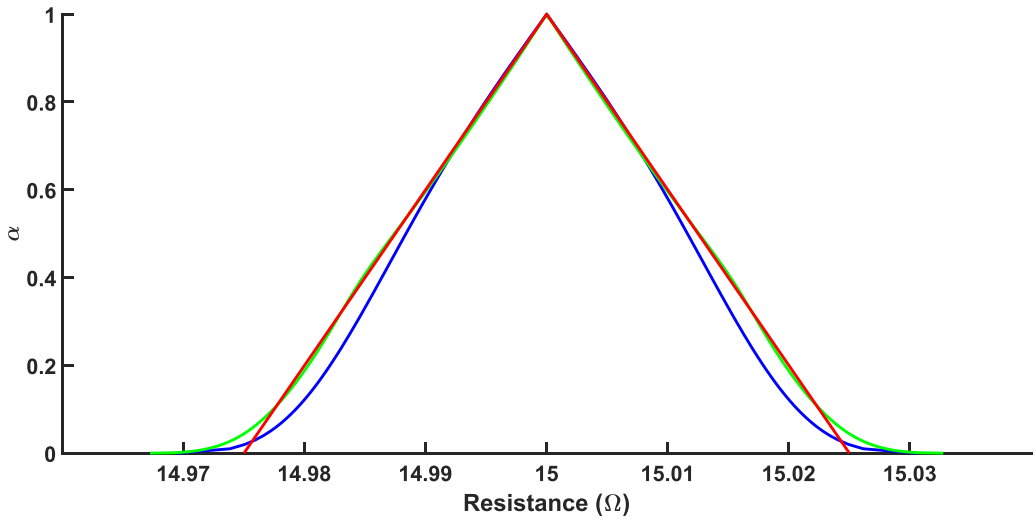

Figure 4. Comparison of the results of the proposed method with those from the blind deconvolution algorithm. Red line: actual X distribution; blue line: obtained X_d distribution by means of the blind deconvolution algorithm; green line: obtained X_d distribution by means of the proposed deconvolution algorithm.

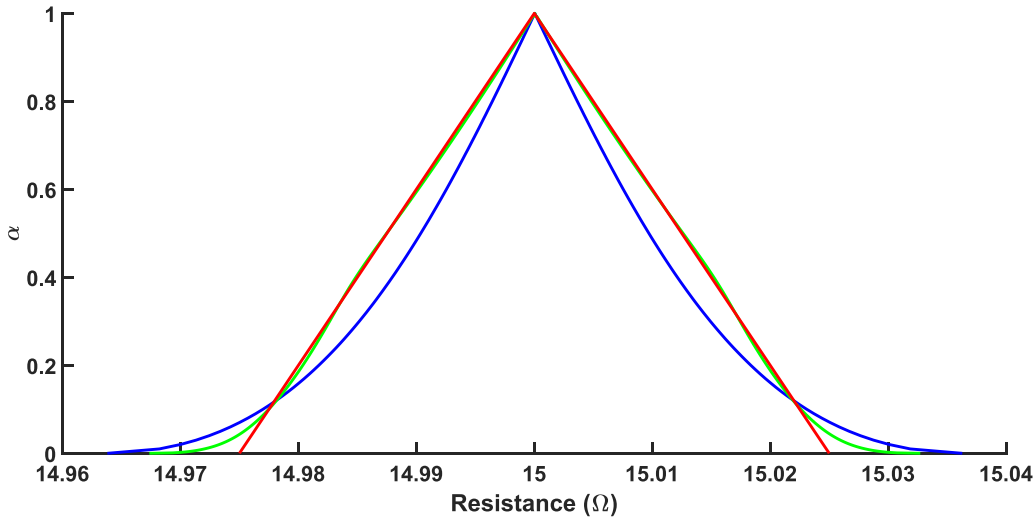

Figure 5. Comparison of the results of the proposed method with those from the Lucy-Richardson deconvolution algorithm. Red line: actual X distribution; blue line: obtained X_d distribution by means of the Lucy–Richardson deconvolution algorithm; green line: obtained X_d distribution by means of the proposed deconvolution algorithm.

Figure 6 shows the result of the comparison of the proposed method with that obtained from the Wiener filter deconvolution algorithm [16, 17].

The red line represents the PD corresponding to the assumed X distribution, the blue line corresponds to the PD obtained from the X_d probability distribution after deconvolution using the Wiener filter deconvolution algorithm, and the green line represents the PD obtained using the proposed algorithm.

It can be clearly seen that the PD obtained using the proposed method is much closer to the actual X distribution than that obtained using the Wiener filter deconvolution.

5.2. Case 2

In case 2, the same case study as case 1 was performed for different distributions. It has been assumed that the manufactured resistors distribute according to a triangular probability distribution centered at 15Ω and with half the base of 0.025Ω.

It has been assumed that the variability S of the measuring instrument has the same uniform probability distribution as the previous case, with a half-width of 0.0125Ω.

It has been assumed once again that 200 000 resistors have been measured using this instrument. So, to simulate the measuring process, the true value of the resistors (R_{true}) was

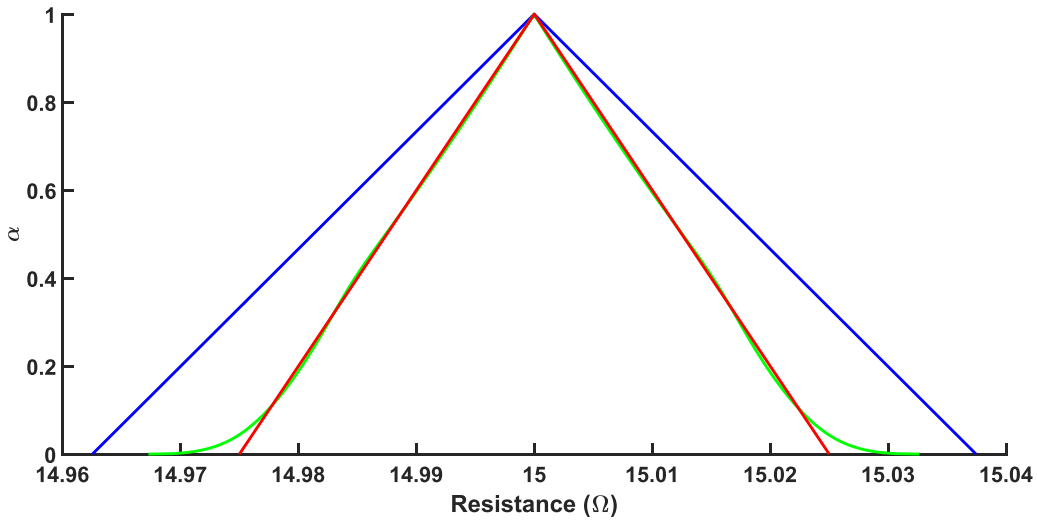

Figure 6. Comparison of the results of the proposed method with those from the Wiener filter deconvolution algorithm. Red line: actual X distribution; blue line: obtained X_d distribution by means of the Wiener filter deconvolution algorithm; green line: obtained X_d distribution by means of the proposed deconvolution algorithm.

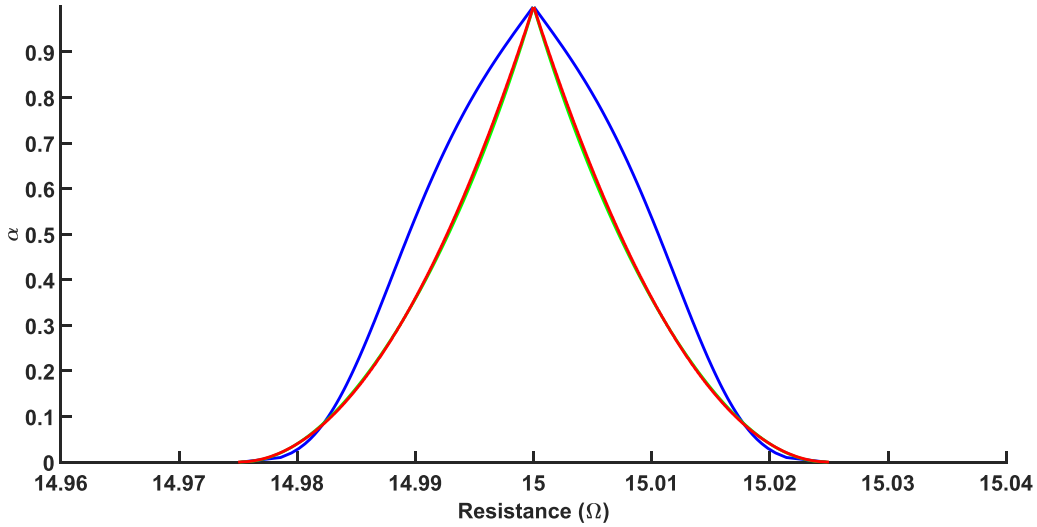

Figure 7. Comparison of the results of the proposed method with those from the blind deconvolution algorithm. Red line: actual X distribution; blue line: obtained X_d distribution by means of the blind deconvolution algorithm; green line: obtained X_d distribution by means of the proposed deconvolution algorithm.

obtained by drawing a random value from distribution X and then the measured value of the resistor is obtained by drawing a random value from the uniform distribution centered at each generated true value of the resistor and with a half-width of 0.0125Ω which is the probability distribution represented by $[R_{\text{true}} - 0.0125; R_{\text{true}} + 0.0125]$.

Therefore, 200 000 measured values have been obtained again and their histogram has been generated to represent the distribution Y of the measurement results and interpolated with a suitable fitting function. Distribution X_d was obtained again from Y and S by applying one of the deconvolution algorithms seen in section 2. All considered PDFs have also been transformed into the corresponding PDs, and the proposed deconvolution algorithm applied.

Figure 7 shows the result of the comparison of the proposed method with that obtained from the blind deconvolution algorithm [11–13].

Just as in the previous case, the red line represents the PD corresponding to the assumed X distribution, the blue line corresponds to the PD obtained from the X_d probability distribution after deconvolution using the blind deconvolution algorithm, and the green line represents the PD obtained using the proposed algorithm.

It can be clearly seen that the PD obtained using the proposed method is much closer to the actual X distribution than that obtained using the blind convolution algorithm.

Figure 8 shows the result of the comparison of the proposed method with that obtained from the Lucy–Richardson deconvolution algorithm [14, 15].

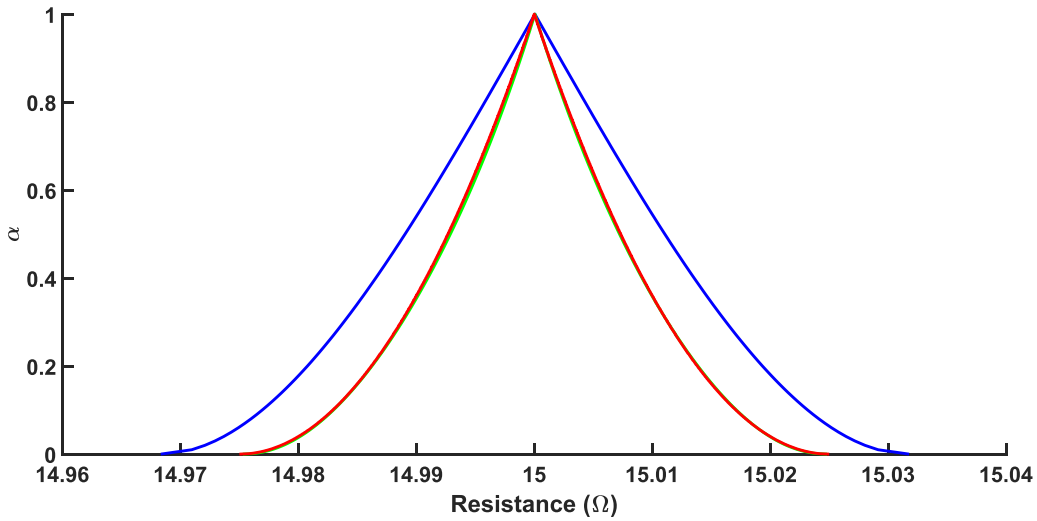

Figure 8. Comparison of the results of the proposed method with those from the Lucy-Richardson deconvolution algorithm. Red line: actual X distribution; blue line: obtained X_d distribution by means of the Lucy–Richardson deconvolution algorithm; green line: obtained X_d distribution by means of the proposed deconvolution algorithm.

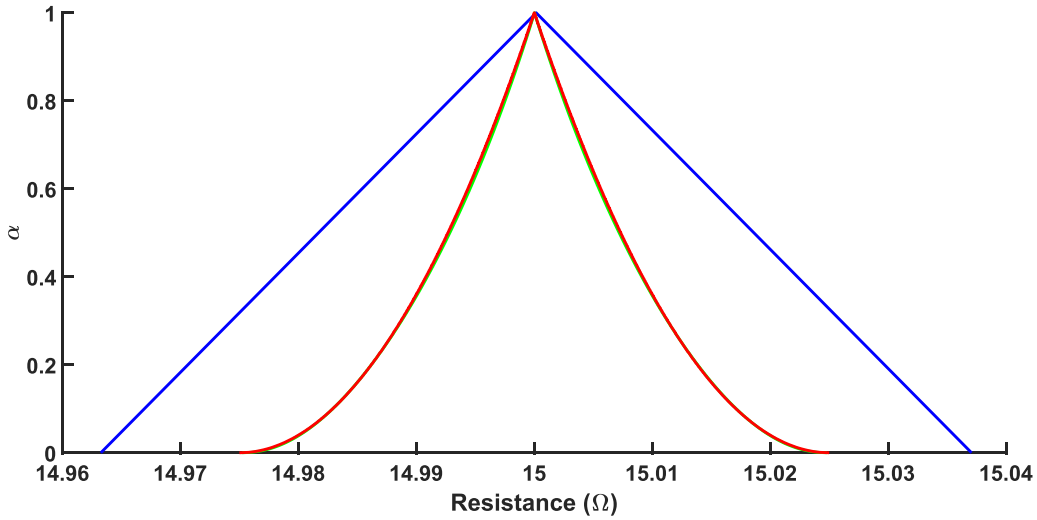

Figure 9. Comparison of the results of the proposed method with those from the Wiener filter deconvolution algorithm. Red line: actual X distribution; blue line: obtained X_d distribution by means of the blind deconvolution algorithm; green line: obtained X_d distribution by means of the proposed deconvolution algorithm.

The red line represents the PD corresponding to the assumed X distribution, the blue line corresponds to the PD obtained from the X_d probability distribution after deconvolution using the blind deconvolution algorithm, and the green line represents the PD obtained using the proposed algorithm.

It can be clearly seen that the PD obtained using the proposed method is much closer to the actual X distribution than that obtained using the blind convolution algorithm.

Figure 9 shows the result of the comparison of the proposed method with that obtained from the Wiener filter deconvolution algorithm [16, 17].

Once again the red line represents the PD corresponding to the assumed X distribution, the blue line corresponds to the PD obtained from the X_d probability distribution after deconvolution using the Wiener filter deconvolution algorithm, and the green line represents the PD obtained using the proposed algorithm.

It can be clearly seen that the PD obtained using the proposed method is much closer to the actual X distribution than that obtained using the Wiener filter deconvolution.

Hence it can be seen from all simulated cases that the proposed method gives much better results than those provided by the existing deconvolution algorithms.

6. Experimental results

To validate the proposed method, the experimental set-up shown in figure 10 was implemented. A signal generator was developed, based on a NI9263 DAC board, featuring four output analog channels with 16-bit resolution, a ± 10 V range,

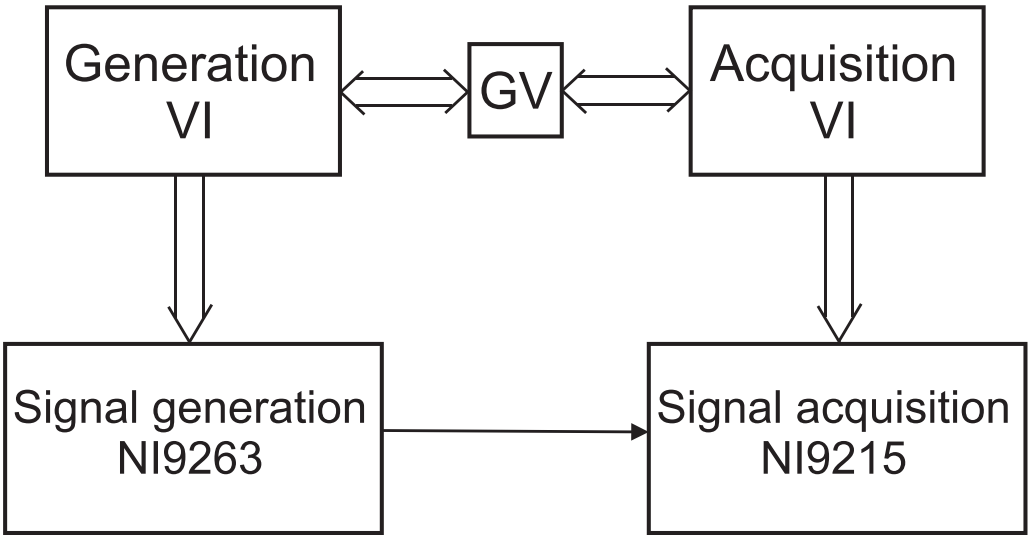

Figure 10. Implemented experimental setup.

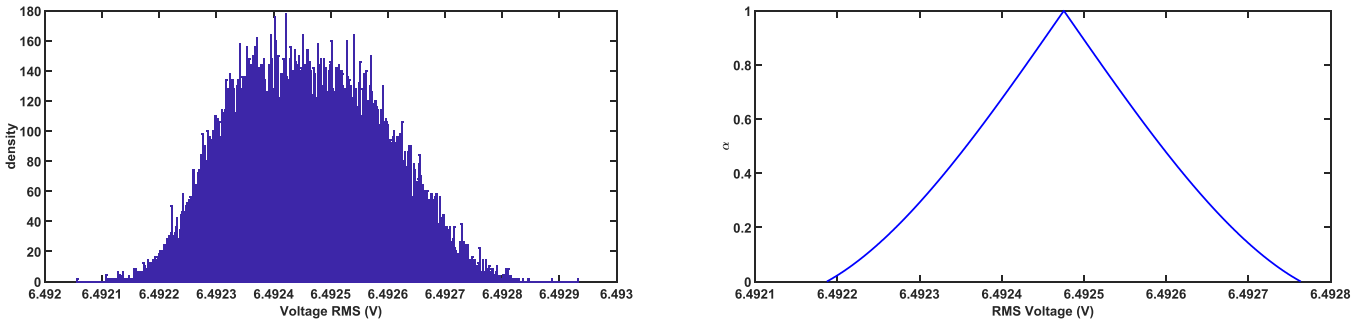

Figure 11. Histogram of the values representing the *S* distributions (a) and corresponding PD (b) obtained by applying the considered p–p transformation.

and a maximum update frequency of 100 kS s^{-1}. Signal generation was controlled by a dedicated generation VI.

The generated signal was then acquired by a NI9215 ADC board, featuring four simultaneous input analog channels with a 16-bit resolution, a ±10 V range, and a maximum sampling rate of 100 kHz on a single channel. The acquisition and subsequent measurement algorithms were controlled by a dedicated VI. Both boards were connected to a NI9174 cRIO chassis, connected to a PC, on which the implemented LabVIEW VIs were running. When needed, the generation and acquisition VIs could be synchronized by means of a LabVIEW Global Variable (GV in the block diagram shown in figure 10).

The experimental validation was conducted according to the two following steps.

- **System characterization.** A pure sinewave was generated by the generation board, with a peak amplitude of 9.18 V and a frequency of 57.005 Hz. 512 samples/period were generated with an update frequency of 29 186.43 Hz. The 57.005 Hz signal frequency was chosen to avoid interference from the 50 Hz frequency of the supply voltage. The generated sinewave was acquired by the acquisition board, with a sampling frequency of 14 593.21 Hz, so that 256 samples/period could be acquired under coherent sampling conditions and spectral leakage errors could be minimized. The acquired samples were then derated to a 12-bit resolution, in order to minimize the influence of the quantization error of the generation board, with respect to the one of the acquisition board.

The sampled data were then processed to evaluate the sinewave rms value over a two-period window. 50 000 repeated measurements were performed, and the distribution of the obtained rms values was considered as the variability *S* of the measuring system. Figure 11(a) shows the histogram of the obtained values, representing the *S* distribution, while figure 11(b) shows the corresponding PD obtained by applying the above mentioned p-p transformation. In such a way, the uncertainty contributions generated by the generation board were attributed to the measuring instrument. Since the same set-up was also used in the second step, when a pre-defined variability was assigned to the peak value of

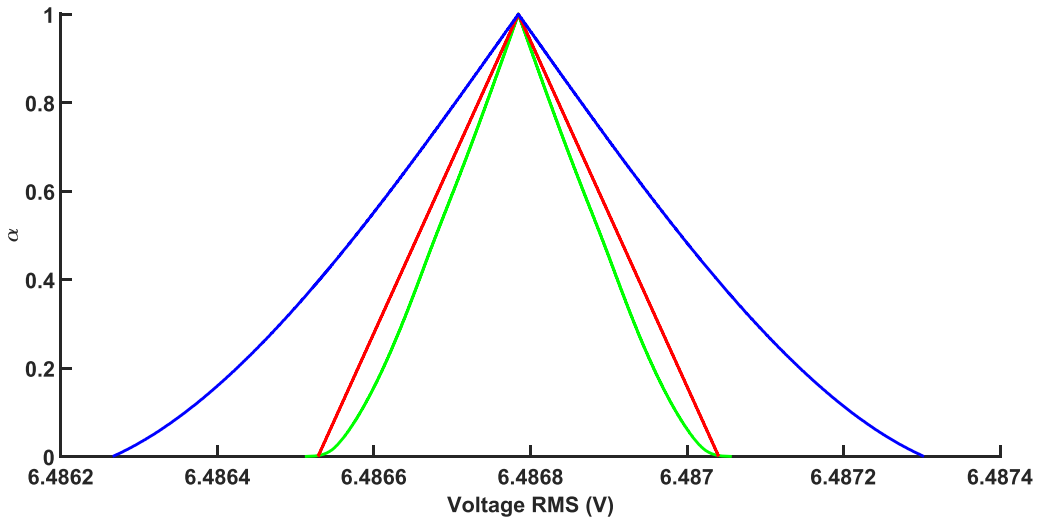

Figure 12. Result provided by the proposed method in case of uniform distribution for X with support 50% larger than that of S. Blue line: PD representing the distribution Y of the measured values. Red line: PD representing the theoretical predefined uniform distribution for the measurand. Green line: PD representing the X_d distribution provided by the implemented deconvolution algorithm.

the generated sinewave, this procedure appears to be suitable to separate the measuring system contribution to the variability of the measured values, from that of the measurand. According to the experimental data, the distribution standard deviation was $\sigma_S = 0.13$ mV and the width of its support, that is the width of the α-cut for $\alpha = 0$ of the corresponding PD, was $W_{\alpha=0} = 0.51$ mV.

- **Variable measurand generation.** In this second step, 50 000 values were generated, according to a pre-defined PDF, for the sinewave peak value, and stored in the generation VI. The same sinewave as in the previous step was then generated with the peak value taken from the stored values and changed every four periods of the generated waveform, thus generating 50 000 sinewaves, each one with a different peak value taken from the given distribution. Once every new sinewave was generated, the global variable was set.

  The acquisition VI was then triggered by the global variable, acquired two periods of the generated sinewave under the same conditions as the ones in the previous step, and evaluated the rms value. The global variable was then reset, so that the procedure could start again with the newly generated sinewave. At the end, 50 000 rms values were available, representing the Y distribution of the measured values, and the proposed deconvolution algorithm could be applied to obtain the variability X of the measurand and compare it with the pre-defined distribution used to generate the peak values.

Two different PDFs have been considered for modeling the variability X of the measurand: a uniform and a triangular distribution. In both cases, the support of the distributions was taken the 50% larger than that of the S distribution in a first experiment, and the same as that of the S distribution in a second experiment.

Figure 12 shows the result provided by the proposed algorithm when the measurand distributes according to a uniform distribution with support 50% larger than that of the distribution of values S that can be attributed to the employed measuring system when the measurand is supposed to not vary. The measured values distribute with a standard deviation, $\sigma_y = 0.315$ mV, and the blue line in figure 12 shows the PD representing the distribution Y of the values returned by the measuring system. The red line shows the PD representing the pre-set X distribution of values assigned to the measurand, while the green line shows the PD representing the X_d distribution provided by the proposed algorithm.

It can be readily checked that the X_d PD approximates very well the pre-set X PD. To provide a quantitative estimate of how well the proposed algorithm provides the measurand variability by deconvolving the Y and S distributions, the rms distance between the X and X_d PDs was computed, and a value of 30.3 μV was obtained.

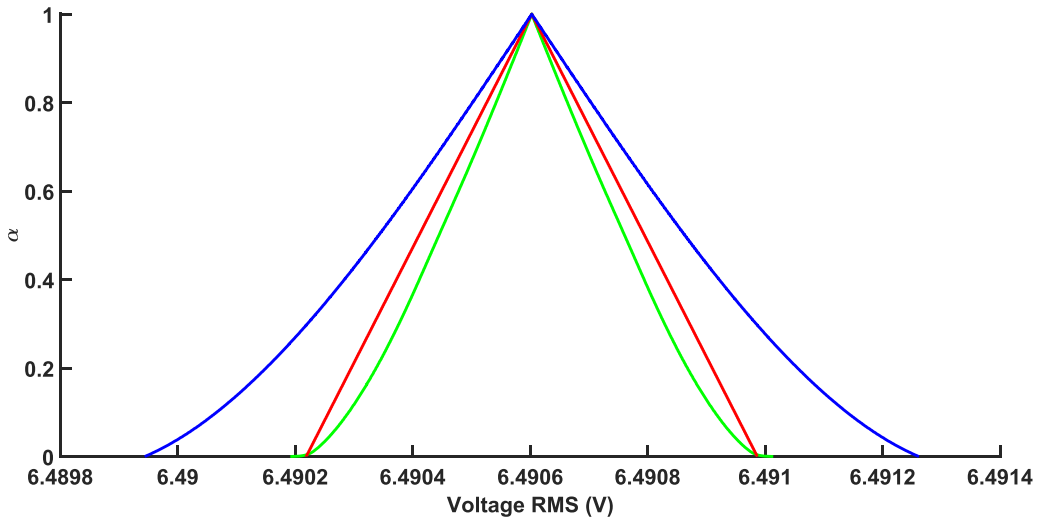

Figure 13. Result provided by the proposed method in case of uniform distribution for X with the same support as that of S. Blue line: PD representing the distribution Y of the measured values. Red line: PD representing the theoretical predefined uniform distribution for the measurand. Green line: PD representing the X_d distribution provided by the implemented deconvolution algorithm.

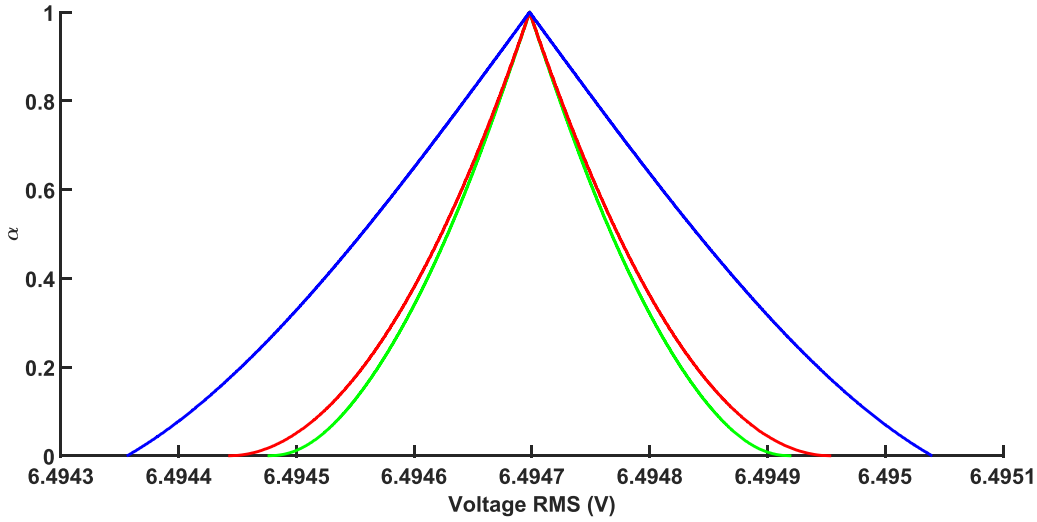

Figure 14. Result provided by the proposed method in case of triangular distribution for X with support 50% larger than that of S. Blue line: PD representing the distribution Y of the measured values. Red line: PD representing the theoretical predefined triangular distribution for the measurand. Green line: PD representing the X_d distribution provided by the implemented deconvolution algorithm.

Figure 13 shows the same results as those shown in figure 12, when the measurand distributes according to a uniform distribution with the same support as that of the distribution of values S that can be attributed to the employed measuring system when the measurand is supposed to not vary. The measured values distribute with a standard deviation $\sigma_y = 0.246V$ mV. Once again, the PD shown by the green line (X_d), returned by the proposed algorithm, appears to be a good approximation of the PD shown by the red line, representing the pre-set X distribution.

The rms distance between the two PDs is, in this case, 22.2 μV, showing that it is possible to extract, from the distribution of the measured values Y, the actual distribution of the measurand even when the variability (S) introduced by the measuring system has a similar value as that of the measurand (X).

Figures 14 and 15 show the same results as those presented in figures 12 and 13 when the measurand distributes according to a triangular distribution, with support that is, respectively, 50% larger and the same as that of the distribution of values S that can be attributed to the employed measuring system when the measurand is supposed to not vary. The measured values distribute with a standard deviation $\sigma_y = 0.236$ mV and $\sigma_y = 0.143$ mV respectively. In both figures, the red and green lines are very close to each other, thus confirming that also in this case the proposed algorithm provides very good results. The rms distance between the two PDs is, respectively, 10.9 μV and 10.5 μV.

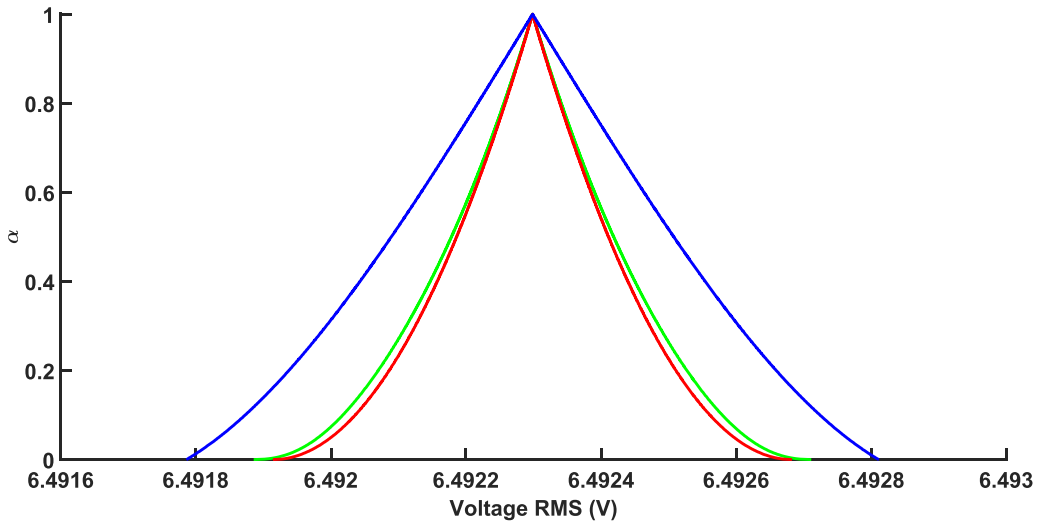

Figure 15. Result provided by the proposed method in case of triangular distribution for X with the same support as that of S. Blue line: PD representing the distribution Y of the measured values. Red line: PD representing the theoretical predefined triangular distribution for the measurand. Green line: PD representing the X_d distribution provided by the implemented deconvolution algorithm.

7. Conclusion

This paper has proposed a method, based on PDs, to perform a deconvolution between two PDFs. In metrology, this method can be usefully applied to separate, in the distribution of measured values, the variability contributions introduced by the measuring system, from the actual variability of the measurand.

While applying this method may appear quite straightforward from a mere theoretical point of view, its practical application may provide quite inaccurate results when the deconvolution is applied to PDFs, as shown by the simulation results. On the contrary, when the PDFs are transformed into equivalent PDs, the deconvolution operation becomes much simpler, application-wise, and provides significantly more accurate results, as proved by both the simulation and experimental results.

In particular the method was experimentally applied to extract the actual variability of the measurand from the distribution of values provided by the employed measuring system, after having evaluated its contribution to variability. The method provided accurate results even when the variability of the measurand was quite similar to that of the employed measuring system, thus making this method quite useful in performing calibration, since it removes the requirement that the uncertainty of the reference be negligible with respect to that of the instrument to be calibrated to ensure that the distribution of the measured value represents the behavior of the instrument to be calibrated. If the proposed method is applied, the variability of the instrument to be calibrated can be separated by that of the reference even when instrument and reference show similar uncertainties.

Data availability statement

The experiment that has been used to obtain the data used in the paper can be replicated very easily with a simple setup. The data that support the findings of this study are available upon reasonable request from the authors.

ORCID iDs

Alessandro Ferrero https://orcid.org/0000-0002-6760-2925
Simona Salicone https://orcid.org/0000-0003-4683-7669
Harsha Vardhana Jetti https://orcid.org/0000-0001-9407-2344
Sina Ronaghi https://orcid.org/0000-0003-2365-5141

References

[1] JCGM 200:2012 2012 International vocabulary of metrology—basic and general concepts and associated terms (VIM 2008 with minor corrections) *Joint Committee for Guides in Metrology*
[2] JCGM 100:2008 2008 Evaluation of measurement data—guide to the expression of uncertainty in measurement, (GUM 1995 with minor corrections) *Joint Committee for Guides in Metrology*
[3] Pou J-M and Leblond L 2018 ISO/IEC guide 98-4: a copernican revolution for metrology *IEEE Instrum. Meas. Mag.* **21** 6
[4] JCGM 106:2012 2012 Evaluation of measurement data—the role of measurement uncertainty in conformity assessment *Joint Committee for Guides in Metrology*
[5] JCGM 101:2008 2008 Evaluation of measurement data—supplement 1 to the Guide to the expression of uncertainty in measurement—propagation of distributions

using a Monte Carlo method *Joint Committee for Guides in Metrology*
[6] Salicone S and Prioli M 2018 *Measurement Uncertainty Within the Theory of Evidence* (*Measurement Science and Technology*) (Springer)
[7] Ferrero A and Salicone S 2018 A comparison between the probabilistic and possibilistic approaches: the importance of a correct metrological information *IEEE Trans. Instrum. Meas.* **67** 607
[8] Ferrero A and Salicone S 2012 Uncertainty: only one mathematical approach to its evaluation and expression? *IEEE Trans. Instrum. Meas.* **61** 2167
[9] Pertile M, De Cecco M and Baglivo L 2010 Uncertainty evaluation in two-dimensional indirect measurement by evidence and probability theories *IEEE Trans. Instrum. Meas.* **59** 2816
[10] Pertile M and De Cecco M 2008 Uncertainty evaluation for complex propagation models by means of the theory of evidence *Meas. Sci. Technol.* **19** 1
[11] Nandi A, Mampel D and Roscher B 1995 Comparative study of deconvolution algorithms with applications in non-destructive testing *IEE Coll. on Blind Deconvolution - Algorithms and Applications* p 1/1–1/6
[12] Lyubchyk L and Grinberg G 2007 Blind deconvolution and separation signal processing via inverse model approach *2007 4th IEEE Workshop on Intelligent Data Acquisition and Advanced Computing Systems: Technology and Applications* pp 325–8
[13] Lifeng K, Pan N and Yi Z 2016 Improved frequency domain blind deconvolution algorithm in acoustic fault feature extraction of bearing *2016 IEEE Int. Conf. on Information and Automation (ICIA)* pp 776–9
[14] Zhong C, Fu J and Ding Y 2011 Image motion compensation for a certain aviation camera based on Lucy-Richardson algorithm *Proc. 2011 Int. Conf. on Electronics and Optoelectronics* vol 4 p V4–141–144
[15] Panfilova K and Umnyashkin S 2016 Linear blur compensation in digital images using Lucy-Richardson method *2016 IEEE NW Russia Young Researchers in Electrical and Electronic Engineering Conf. (EIConRusNW)* pp 302–4
[16] Yang L, Zhang X and Ren J 2011 Adaptive wiener filtering with Gaussian fitted point spread function in image restoration *2011 IEEE 2nd Int. Conf. on Software Engineering and Service Science* pp 890–4
[17] Khetkeeree S and Liangrocapart S 2019 Image restoration using optimized weiner filtering based on modified Tikhonov regularization *2019 IEEE 4th Int. Conf. on Signal and Image Processing (ICSIP)* pp 1015–20
[18] Shafer G 1976 *A Mathematical Theory of Evidence* (Princeton University Press)
[19] Klir G J and Yuan B 1995 *Fuzzy Sets and Fuzzy Logic. Theory and Applications* (Prentice Hall PTR)
[20] Alsina C, Schweizer B and Frank M J 2006 *Associative Functions: Triangular Norms and Copulas* (World Scientific)
[21] Klement E P, Mesiar R and Pap E 2004 Triangular norms. Position paper I: basic analytical and algebraic properties *Fuzzy Sets Syst.* **143** 5
[22] Klement E P, Mesiar R and Pap E 2004 Triangular norms. Position paper II: general constructions and parameterized families *Fuzzy Sets Syst.* **145** 411
[23] Klement E P, Mesiar R and Pap E 2000 *Triangular Norms* (Kluwer)
[24] Alsina C, Frank M J and Schweizer B 2006 *Associative Functions: Triangular Norms and Copulas* (World Scientific)
[25] Ferrero A, Prioli M, Salicone S and Vantaggi B 2012 2D probability-possibility transformations *SMPS 2012 (Konstanz, Germany, 4–6 October)*
[26] Ferrero A, Prioli M, Salicone S and Vantaggi B 2013 A 2-D metrology-sound probability-possibility transformation *IEEE Trans. Instrum. Meas.* **62** 1–9
[27] Dubois D, Foulloy L, Mauris G and Prade H 2004 *Reliable Computing* vol 10 (Kluwer Academic Publishers) p 273
[28] Klir G J and Geer J F 1993 *Fuzzy Logic* (*Theory and Decision Library* vol 12) ed R Lowen and M Roubens (Springer) pp 417–28
[29] Dombi J 2008 Towards a general class of operators for fuzzy systems *IEEE Trans. Fuzzy Syst.* **16** 477